X-ray diffraction study of stress relaxation in cubic boron nitride films grown with simultaneous medium-energy ion bombardment

B. Abendroth,[a] R. Gago, F. Eichhorn, and W. Möller
Institute of Ion Beam Physics and Materials Research, Forschungszentrum Rossendorf, PF 510119, 01314 Dresden, Germany

(Received 26 July 2004; accepted 19 October 2004)

Relaxation of the intrinsic stress of cubic boron nitride (*c*BN) thin films has been studied by x-ray diffraction (XRD) using synchrotron light. The stress relaxation has been attained by simultaneous medium-energy ion bombardment (2–10 keV) during magnetron sputter deposition, and was confirmed macroscopically by substrate curvature measurements. In order to investigate the stress–release mechanisms, XRD measurements were performed in in-plane and out-of-plane geometry. The analysis shows a pronounced biaxial state of compressive stress in the *c*BN films grown without medium-energy ion bombardment. This stress is partially released during the medium-energy ion bombardment. It is suggested that the main path for stress relaxation is the elimination of strain within the *c*BN grains due to annealing of interstitials. © *2004 American Institute of Physics*. [DOI: 10.1063/1.1836868]

Cubic boron nitride (*c*BN) is, next to diamond, the second hardest material known. In contrast to diamond, *c*BN does not react with ferrous metals and is stable against oxidation up to 1300 °C.[1] Thus, *c*BN is a very promising material for tribological applications. The growth of *c*BN films has been demonstrated using a variety of physical and chemical vapor deposition processes (for detailed review articles, see Refs. 1 and 2). In general, all deposition processes have in common that a low-energy ion bombardment (~100–500 eV) is required for the nucleation and growth of the *c*BN.[3] As a consequence of this low-energy ion bombardment, the films exhibit very high intrinsic compressive stress (exceeding −10 GPa), which limits the adhesion and the maximum film thickness.[1]

In order to reduce the stress in *c*BN films, several relaxation methods have been reported.[4] Among them, a promising option is the use of ion implantation into regions well below the film surface (30 keV–1 MeV).[5,6] Following this approach, the combination of sequential *in situ* ion implantation and film growth has been shown as a method to produce thick films (>1 μm).[7] This study has been extended to simultaneous medium-energy ion implantation during the growth by ion beam assisted deposition[8,9] and magnetron sputtering (MS).[10] In these investigations, it was found that the stress relaxation is controlled by the flux and energy of the medium-energy ions implanted during the growth. Particularly, the amount of stress release correlates with the number of atomic displacements generated by the medium-energy ion impacts.

Postdeposition annealing has also been demonstrated to reduce stress in *c*BN thin films,[11,12] but is less efficient than ion implantation.[6,12] Annealing additional to medium-energy ion implantation, however, was found to reduce efficiently the structural degradation, which accompanies the ion implantation process.[6,13]

Despite the effective stress release upon medium-energy ion bombardment, the relaxation mechanisms are not well identified. One way to quantify the film stress evolution and to monitor the stress relaxation during the film growth is to measure *in situ* the substrate curvature during deposition by means of laser deflection.[14] However, the measurement of the substrate curvature yields the film stress on a macroscopic level (sum of intrinsic, interface, and thermal stresses), which makes it difficult to discern between the contribution of different relaxation mechanisms. The aim of this work was to study the stress relaxation induced by simultaneous medium-energy ion bombardment during the growth by MS on an atomic scale by means of x-ray diffraction (XRD) using high-brilliance synchrotron radiation and, in this way, identify possible mechanisms involved.

The *c*BN thin films were prepared by radio frequency MS in Ar/N_2 (35% and 100% N_2) discharge. A negative dc substrate bias (−150 V) in combination with negative high voltage (HV) pulses (2–8 kV) were used to enable *c*BN nucleation and growth and simultaneously achieve stress relaxation. Prior to the nucleation of *c*BN, a ~50 nm hexagonal BN (*h*BN) buffer layer was deposited to improve the adhesion and the total film thickness was 150 nm. For comparison, one sample was produced without medium-energy ion bombardment. To prevent delamination, the total thickness of this sample was limited to ~50 nm. The evolution of the stress during deposition was monitored with *in situ* substrate bending measurements by laser deflection. The details of sample preparation and *in situ* stress measurement are given in Ref. 10.

The value of residual stress for the films considered in this work and the preparation parameters are shown in Table I. The data show a clear correlation between the stress level and the amount of ion damage induced by the medium-energy ions. The dynamic ion damage that is produced during the HV pulses is expressed in terms of displacements per atom (dpa). The number of dpa was calculated for each sample from the total number of displacements per incoming ion as obtained by SRIM[15] (with the energy of N^+ being one-half of that of Ar^+), the ion flux, which depends on the HV pulse frequency, and the growth rate (5 nm/s). Additionally, a sample prepared with medium-energy ion implantation (1.2

[a]Author to whom correspondence should be addressed; electronic mail: b.abendroth@fz-rossendorf.de

TABLE I. Medium-energy ion bombardment parameters during MS deposition and the computed ion-induced damage. The measured intrinsic stress values derived from *in situ* cantilever bending are also included and correlate with the degree of ion-induced damage.

Pulse voltage (kV)	Pulse frequency (kHz)	Stationary damage (dpa)	Stress (GPa)	Comments
		0	-9.0 ± 0.1	*c*BN with high stress
-8	2.8	0.5	-2.6 ± 0.1	100% N_2 discharge
-4	2.8	0.7	-1.7 ± 0.1	$Ar+N_2$ discharge
-8	2.8	1.2	-1.6 ± 0.1	$Ar+N_2$ discharge
-8	2.8	1.2	⋯	$Ar+N_2$ discharge annealing at 900 °C

dpa) was annealed at 900 °C after deposition as a reference sample with no or very low stress.

XRD measurements were performed at the ROssendorf Beam Line (ROBL)[16] at the European Synchrotron Radiation Facility (ESRF). The experiments were done under grazing incidence to minimize the signal coming from the Si substrate. The wavelength of the incident x-ray was 1.2 Å (10.3 keV) and the angle of incidence (θ) was set to 0.2°, slightly above the critical angle for total internal reflection ($\alpha_c = 0.19°$) to enhance the intensity of the signal. For each sample, in-plane (2ω) and out-of-plane (2θ) scans were performed. In this way, lattice planes oriented perpendicular and parallel, respectively, to the surface can be detected and a biaxial stress in the samples can be mapped.

Figure 1 shows the data recorded in-plane [Fig. 1(a)] and out-of-plane [Fig. 1(b)] detector scans for *c*BN samples produced with different medium-energy ion damage. The sample grown without HV pulses [lowest curve in Figs. 1(a) and 1(b)] is used as a reference representing a nonrelaxed *c*BN film and, hence, with high compressive stress. In the in-plane geometry, the Bragg peaks related to the *h*BN (002) and *c*BN (111) reflections are identified. The *h*BN signal originates mainly from the *h*BN buffer layer. In the out-of-plane geometry, the *h*BN (002) peak vanishes due to the preferential orientation of this buffer layer with the *c* axis parallel to the substrate, which is typical for *h*BN grown under low-energy ion bombardment.[17] The *c*BN (111) diffraction peak in all samples is more intense in the out-of-plane than in-plane scan, indicating a preferential orientation of the *c*BN(111) planes parallel to the surface. This texture is more pronounced in the sample grown without HV pulses (nonrelaxed) and it is attenuated with the addition of medium-energy ion bombardment.

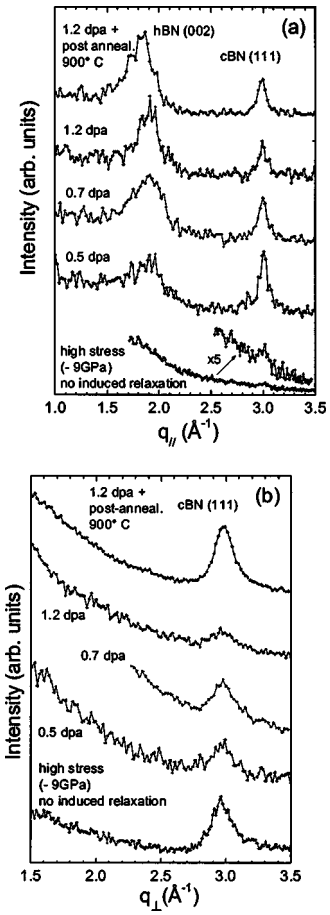

FIG. 1. In-plane (a) and out-of-plane (b) diffraction pattern of BN thin films with different ion-induced damage and stress relaxation. The in-plane spectrum of the nonreleased sample shows a very low intensity due to the small film thickness (50 nm).

Figure 2 shows the *c*BN (111) lattice distances, $d(111)$, obtained from the fitting of the diffraction patterns of Fig. 1. Due to the high texture for the sample grown without HV pulses and its low thickness, the error in the fitted in-plane *c*BN(111) peak position is larger than for the other samples. For comparison, the tabulated $d(111)$ value of polycrystalline *c*BN (Ref. 18) is also included. Even under compressive stress, the in-plane $d(111)$ values from the *c*BN films are larger than for the *c*BN powder reference. This is most likely due to the nanocrystalline structure and incorporation of defects as a result of the deposition process. The $d(111)$ interplanar distance is larger in the out-of-plane than in the in-plane direction, indicating a pronounced biaxial state of

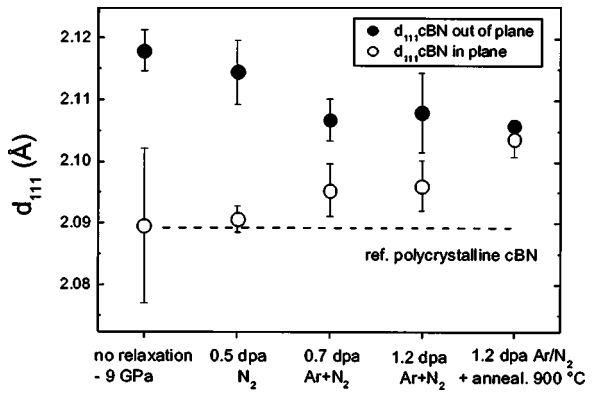

FIG. 2. *c*BN (111) lattice spacing measured in the in-plane (●) and out-of-plane (○) geometries for samples with different degrees of ion-induced damage and stress relaxation. For comparison, the values of polycrystalline *c*BN, a nonrelaxed *c*BN thin film and a *c*BN thin film that is stress free after annealing at 900 °C are shown.

compresive stress. For the additionally annealed sample, the isotropic lattice spacing, with equal in-plane and out-of-plane values, indicates a complete relaxation of the structure. Upon the thermal treatment, apart from annealing of defects, the residual stress can also be partially accumulated at the interface due to the fact that above 600 °C plastic deformation occurs in the Si substrate.[19] In any case, the results show that the combination of postannealing and medium-energy ion bombardment can be efficiently used to produce stress-free *c*BN by MS. For the samples grown under medium-energy ion bombardment, the in-plane and out-of-plane $d(111)$ distances converge toward the value of the annealed sample with increasing ion-induced damage, in agreement with the macroscopic stress values displayed in Table I. This is a clear indication that the ion bombardment leads to a strain relaxation at an atomic scale and within the *c*BN grains.

The size of the *c*BN grains is ~3 nm and ~6 nm for the out-of-plane and in-plane directions, respectively, as determined from the full width at half maximum of the *c*BN (111) reflection. These values are neither affected by the ion bombardment nor by the annealing procedure, the latter in agreement with the observations by Donner *et al.*[11] Hence, it can be stated that the medium-energy ion bombardment neither induces an amorphization nor a phase transformation of the *c*BN crystalline grains. High stability of the *c*BN phase against ion bombardment has also been reported by Eyhusen *et al.*[20] Therefore, the observed macroscopic stress relaxation is mainly caused by a strain relaxation due to the removal of point defects within the *c*BN grains and not by a phase transformation into *h*BN. This process is likely the result of the thermal spikes induced by the medium-energy ion impacts, where the ratio of formed defects and annealed defects is very low for the considered ion energies.[21] The thermal spikes are also implied in the analytical model of ion-induced stress formation in thin films by Davis,[22] to explain the stress reduction at higher ion energies. Therefore, the stress in the *c*BN is effectively released by the medium energy-ion bombardment, although additional displacements are introduced.

Complementary to the results presented in this letter, infrared (IR) spectroscopy revealed a significant increase of *h*BN for ion damage values exceeding 1 dpa.[10] This phase transformation is not detected in the XRD analysis and could be understood considering the presence of a x-ray amorphous phase with mixed sp^2/sp^3 bonding that is less stable upon ion bombardment than the nanocrystaline *c*BN grains. In fact, it has been shown that a mixture of sp^2/sp^3 phases is not stable upon ion irradiation and transformation towards sp^2 occurs above a certain ion dose threshold.[20] Therefore, the increase in the *h*BN content detected by IR spectroscopy for large dpa must be attributed to a phase transformation in the amorphous matrix and not to a decrease of the *c*BN crystalline phase. In any case, this phase transformation can be minimized by using working conditions leading to an ion damage below the threshold value (1 dpa) while inducing a similar amount of stress relaxation, as shown in Fig. 2. The results also indicate that the optimum ion-damage threshold could be increased and the relaxation process be more efficient by enhancing the crystallinity of the *c*BN phase during the growth.

In conclusion, XRD analysis has shown that effective stress relaxation in *c*BN thin films upon simultaneous medium-energy ion bombardment during the growth process takes place at an atomic scale. The crystalline *c*BN phase is very stable under ion bombardment and the stress relaxation occurs within the *c*BN grains. The main path of stress relaxation seems to be annihilation of interstitials and atomic rearrangements as a result of the thermal spikes induced by the medium-energy bombardment. However, additional post-deposition annealing is required for complete relaxation of the structure. The stress relaxation process could be more efficient by operation under conditions leading to a higher crystallinity of the *c*BN phase.

The authors would like to acknowledge the financial support from the ESRF for the synchrotron experiments under Project No. ME-706. The help of Dr. N. Schell as a local contact and the technical assistance of U. Strauch at ROBL are also much appreciated. The work at FZR has been supported by Deutsche Forschungsgemeinschaft (DFG) under Contract No. FU 303/2-2.

[1] P. B. Mirkarimi, K. F. McCarty, and D. L. Medlin, Mater. Sci. Eng., R. **21**, 47 (1997).
[2] W. Kulisch and S. Ulrich, Thin Solid Films **423**, 183 (2003).
[3] H. Hofsäss, S. Eyhusen, and C. Ronning, Diamond Relat. Mater. **13**, 1103 (2004).
[4] J. Ullmann, A. J. Kellock, and J. E. E Baglin, Thin Solid Films **341**, 238 (1999).
[5] J. Ullmann, J. Baglin, and E. Kellock, J. Appl. Phys. **83**, 2980 (1998).
[6] C. Fitz, W. Fukarek, and W. Möller, Thin Solid Films **408**, 155 (2002).
[7] H.-G. Boyen, P. Widmayer, D. Schwertberger, N. Deyneka, and P. Ziemann, Appl. Phys. Lett. **76**, 709 (2000).
[8] C. Fitz, A. Kolitsch, W. Möller, and W. Fukarek, Appl. Phys. Lett. **80**, 55 (2002).
[9] R. Gago, M. Vinnichenko, B. Abendroth, A. Kolitsch, and W. Möller, J. Vac. Sci. Technol. A **21**, 1739 (2003).
[10] B. Abendroth, R. Gago, A. Kolitsch, and W. Möller, Thin Solid Films **447**, 131 (2004).
[11] W. Donner, H. Dosch, S. Ulrich, H. Erhardt, and D. Abernathy, Appl. Phys. Lett. **73**, 777 (1998).
[12] C. Fitz, A. Kolitsch, and W. Fukarek, Thin Solid Films **389**, 173 (2001).
[13] X. W. Zhang, H.-G. Boyen, P. Ziemann, M. Ozawa, F. Banhardt, and M. Schreck, Diamond Relat. Mater. **13**, 1144 (2004).
[14] C. Fitz, W. Fukarek, A. Kolitsch, and W. Möller, Surf. Coat. Technol. **128**, 474 (2000).
[15] J. Ziegler, J. Biersack, and U. Littmark, *The Stopping and Range of Ions in Solids* (Pergamon, New York, 1985).
[16] W. Matz, N. Schell, G. Bernhard, F. Prokert, T. Reich, J. Claußner, W. Oehme, R. Schlenk, S. Dienel, H. Funke, F. Eichhorn, M. Betzl, D. Pröhl, U. Strauch, G. Hüttig, H. Krug, W. Neumann, V. Brendler, P. Reichel, M. A. Denecke, and H. Nitsche, J. Synchrotron Radiat. **6**, 1076 (1999).
[17] D. L. Medlin, T. A. Friedmann, P. B. Mirkarimi, P. Rez, M. J. Mills, and K. F. McCarty, J. Appl. Phys. **76**, 295 (1994).
[18] Joint Committee on Powder Diffraction Standards (JCPDS) pattern 25-1033.
[19] K. Yasutake, J. Murakami, M. Umeno, and H. Kawabe, Jpn. J. Appl. Phys., Part 2 Part 2 **21**, L288 (1982).
[20] S. Eyhusen, I. Gerhards, H. Hofsäss, C. Ronning, M. Blomenhofer, J. Zweck, and M. Seibt, Diamond Relat. Mater. **12**, 1877 (2003).
[21] F. Seitz and J. Koehler, Solid State Phys. **3**, 305 (1956).
[22] C. Davis, Thin Solid Films **226**, 30 (1993).